

Electronic properties of ferroelectric BaTiO₃/MgO capacitors on GaAs

T. E. Murphy, D. Chen, and J. D. Phillips^{a)}

Department of Electrical Engineering and Computer Science, University of Michigan, Ann Arbor, Michigan 48109-2122

(Received 24 May 2004; accepted 10 August 2004)

Thin films of MgO and BaTiO₃ were deposited on (001) GaAs substrates using molecular beam epitaxy and pulsed laser deposition, respectively. X-ray diffraction scans indicate crystalline MgO and BaTiO₃ thin films with preferential *c*-axis orientation. Capacitors fabricated from the BaTiO₃/MgO/GaAs structures demonstrate ferroelectric hysteresis behavior with a remanent polarization of 0.4 $\mu\text{C}/\text{cm}^2$. Small-signal capacitance measurements indicate an effective dielectric constant for the BaTiO₃/MgO structure of 45.5 ϵ_0 . A hysteresis behavior indicative of ferroelectric switching is observed in the capacitance–voltage characteristics with a memory window of approximately 2 V. The observation of ferroelectric behavior in these materials are promising for future multifunctional devices on GaAs. © 2004 American Institute of Physics.

[DOI: 10.1063/1.1804237]

The integration of oxide materials on GaAs has been sought for decades in the goal of achieving metal-oxide-semiconductor field-effect transistors (MOSFETs). High-quality insulating oxides have been demonstrated using Ga₂O₃ and Gd₂O₃, resulting in GaAs MOSFET devices.^{1,2} The successful integration of oxide materials on GaAs is also sought for optoelectronics applications, where the achievement of aluminum oxide through the wet oxidation of AlGaAs (Ref. 3) has had a major impact on vertical cavity surface-emitting lasers and optical waveguide devices. Electronic, optoelectronic, and future multifunctional devices could benefit enormously from the properties provided by ferroelectric oxides. In particular, ferroelectric oxides possess a switchable polarization, strong electro-optic properties, tunable dielectric constant, and piezoelectric properties. Ferroelectric oxides in the perovskite structure, such as BaTiO₃, have a cubic crystal structure compatible for GaAs integration. However, the integration of perovskite oxides with GaAs is challenging due to the requirements of elevated growth temperatures, significant lattice mismatch, and incompatibility of arsenic with the oxides and oxygen with GaAs. MgO provides a potential means of facilitating the integration of perovskite oxides on GaAs, where there is a near 4:3 commensurate lattice match, low MgO deposition temperatures, and an excellent interdiffusion barrier in MgO.

Previously, high quality cube-on-cube oriented (001) MgO films on (001) GaAs at low growth temperatures ($\sim 350^\circ\text{C}$) have been achieved by pulsed laser deposition,^{4,5} electron beam evaporation,⁶ and molecular beam epitaxy using molecular oxygen.⁷ Due to the large mismatch in the thermal expansion coefficient between GaAs ($\alpha = 5.73 \times 10^{-6}/\text{K}$ at 300 K) and MgO ($\alpha = 11.15 \times 10^{-6}/\text{K}$ at 300 K),⁸ the thickness of MgO buffer layers on GaAs should be minimized. Requirements of thin layers and control over the oxygen-sensitive GaAs/MgO interface suggests that growth techniques such as molecular beam epitaxy are best suited to provide the desired properties for MgO buffer layers. The growth of MgO by molecular beam epitaxy, and subsequent deposition of BaTiO₃ by pulsed laser deposition are de-

scribed in this Letter. The electrical properties of metal-ferroelectric-insulator-semiconductor capacitors fabricated from these materials are described.

MgO was grown on GaAs by molecular beam epitaxy using an elemental magnesium effusion cell and an electron cyclotron resonance (ECR) source for oxygen (2.45 GHz, 250 W). Previous experiments have reported that a high oxygen flux is required to prevent the growth of three-dimensional features from a Mg-GaAs reaction and a subsequent polycrystalline growth of MgO with rough surface morphology.⁷ The use of atomic oxygen here is expected to provide a greater benefit in this respect than molecular oxygen. A Si-doped (n^+) GaAs (001) substrate was heated to 600 °C to desorb the native oxide. *In situ* reflection high-energy electron diffraction (RHEED) was used to monitor the surface. After observing a clear (2×4) reconstruction by RHEED, the substrate was cooled to 350 °C. MgO growth was initiated with 1 SCCM (cubic centimeter per minute at STP) of O₂ flowing and the ECR source set at 90 mA. Growth was continued for 2 h during which time the RHEED pattern corresponding to the GaAs surface slowly diffused and transitioned to a streaky pattern indicative of a MgO (001) surface. The MgO layer thickness was determined to be 16±1 nm from spectroscopic reflectance measurements. After the growth of the MgO layer, half of the sample was loaded into a vacuum chamber for the deposition of BaTiO₃. BaTiO₃ was deposited by pulsed laser deposition using an excimer laser ($\lambda = 248$ nm, 25-ns pulse width, 10 Hz, ~ 2 J/cm²) at a substrate temperature of 600 °C. The thickness of the BaTiO₃ layer was determined to be 150 nm from spectroscopic reflectance measurements. X-ray diffraction measurements (θ -2 θ scan) indicate predominantly *c*-axis-oriented thin films, as shown Fig. 1. A weak reflection at 43° is observed and is consistent with MgO (001). The weak intensity may be attributed to the small thickness of the MgO layer. Peaks observed at 22.2° and 45.3° are consistent with BaTiO₃ (001) and (002) reflections.

Metal-oxide-semiconductor (MOS) capacitors were fabricated on the MgO/GaAs and BaTiO₃/MgO/GaAs samples by depositing Ti/Pt/Au(20/100/200 nm) electrodes with a diameter of 250 μm using a shadow mask. Current–voltage

^{a)}Electronic mail: jphilli@engin.umich.edu

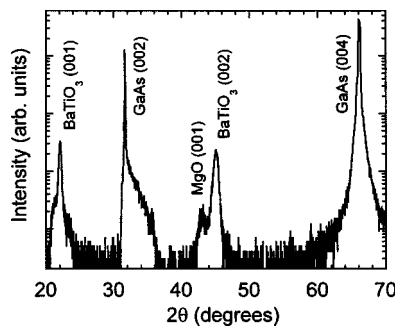


FIG. 1. X-ray diffraction scans of (a) the 16-nm-thick MgO layer on GaAs (100) and (b) the BaTiO₃/MgO/GaAs structure.

characteristics of the metal/MgO/GaAs capacitors show a blocking behavior with a breakdown voltage of approximately 4 V in both forward and reverse directions, with a leakage current of 90 nA. The differential small signal capacitance was measured using a Boonton 72B capacitance meter with a 1-MHz test signal. The differential capacitance–voltage (C – V) characteristics of the metal/MgO/GaAs capacitors are shown in Fig. 2, and are typical of MOS structures on n -type material. A shallow turn-on is observed which may be a result of MgO/GaAs interface states. Previous C – V studies on MgO/GaAs had shown a clockwise hysteresis attributed to “slow” trapping states.⁵ Such hysteresis behavior was not discernable in our measurements. The saturation value of capacitance at positive voltages is in the accumulation region and represents the oxide capacitance $C_{ox} = \epsilon_{ox}A/d_{ox}$, where ϵ_{ox} is the dielectric constant of the oxide, A is the area of the capacitor, and d_{ox} is the oxide thickness. The observed value of $C_{ox} = 255$ pF suggests a value of $\epsilon_{MgO} = 9.4 \pm 0.6\epsilon_0$ (based on the estimated error in determining the MgO thickness) similar to the bulk value of $\epsilon_{MgO} = 9.8\epsilon_0$.

The electrical characteristics of several (~ 15) metal/BaTiO₃/MgO/GaAs capacitors were measured. Approximately 20% of the capacitors were shorted where material defects could be observed. The characteristics of working capacitors had a variation in performance of approximately 10%–20% which may be attributed to nonuniformity in materials properties or layer thickness. The metal/BaTiO₃/MgO/GaAs capacitors show an insulating behavior with leakage currents less than 1 nA. The leakage current for these capacitors becomes significant above ± 4 V. The polarization versus applied voltage (P – V) characteristics were measured using a Radiant Technologies 66A Ferroelectric Test System.

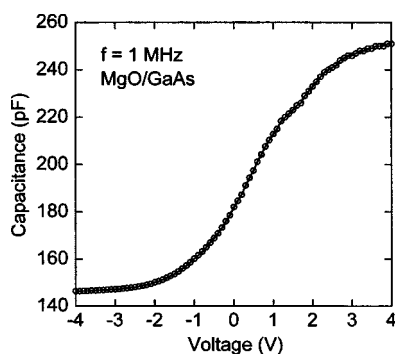


FIG. 2. Capacitance–voltage characteristics of a metal/MgO/GaAs capacitor.

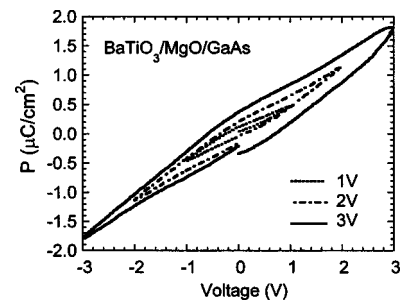


FIG. 3. Polarization vs applied voltage for a metal/BaTiO₃/MgO/GaAs capacitor under a 1-, 2-, and 3-V bias range.

The P – V characteristics for varying applied voltage are shown in Fig. 3 for applied voltages of 1, 2, and 3 V, where P – V curves become distorted at and above 4 V due to the leakage current. A nonsaturating P – V loop is observed with a remanent polarization of $\sim 0.4 \mu\text{C}/\text{cm}^2$ for a 3-V loop. The P – V characteristics are similar in shape and magnitude to previous metal-ferroelectric-insulator-semiconductor reports of SrBi₂Ta₂O₉ on silicon⁹ and SrBi₂Ta₂O₉ on GaAs.¹⁰ Previous experiments on BaTiO₃ thin films deposited on Pt/SiO₂/Si substrates using the equipment and procedures outlined above have resulted in ferroelectric capacitors with larger values of remanent polarization ($> 2 \mu\text{C}/\text{cm}^2$). The reduced polarization values may be a result of nonoptimal deposition conditions or remaining interdiffusion problems associated with the oxide/GaAs interface. Previous experiments on BaTiO₃ thin films deposited (equipment and procedure as outlined above) on GaAs (001) using MgO buffer layers deposited by pulsed laser deposition resulted in no observable hysteresis behavior. The improved ferroelectric behavior observed in this work is likely a result of the improved quality of the MgO/GaAs interface and buffer layer using MBE.

The capacitance–voltage characteristics of the metal/BaTiO₃/MgO/GaAs capacitors are shown in Fig. 4. C – V characteristics were measured in the forward and reverse direction after holding the sample at -5 and $+5$ V, respectively, for several minutes. The oxide capacitance is determined to be 119 pF, resulting in an effective dielectric constant of $45.5\epsilon_0$ for the BaTiO₃/MgO dielectric stack. The values obtained outside of the range of -4 to $+4$ V were determined to be artificially large due to the leakage current, and are therefore not shown. An anticlockwise hysteresis is clearly observed in the C – V characteristics with a voltage shift or “memory window” of approximately 2 V. The

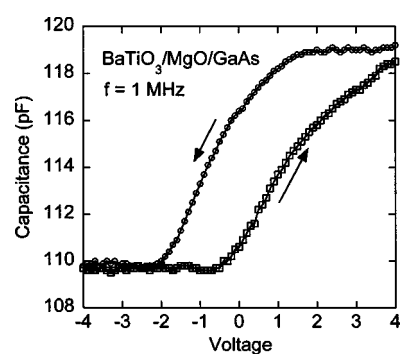


FIG. 4. Capacitance–voltage characteristics of a metal/BaTiO₃/MgO/GaAs capacitor demonstrating hysteresis.

anticlockwise direction of the hysteresis is consistent with switching polarization in a ferroelectric, as opposed to slow trap states at an interface. The existence of such a sizable memory window given a small measured remanent polarization is consistent with the earlier theoretical prediction that the window is primarily determined by the coercive field.¹¹

In conclusion, MgO buffer layers and BaTiO₃ thin films were deposited on *n*-type GaAs. The thin films show a crystalline structure with a predominantly *c* axis orientation. The *C*-*V* characteristics of capacitors using only MgO buffer layers demonstrate insulating behavior and a dielectric constant similar to bulk MgO. Capacitors incorporating BaTiO₃/MgO show ferroelectric *P*-*V* hysteresis with unsaturated behavior and a small remanent polarization. The *C*-*V* characteristics of the BaTiO₃/MgO capacitors show ferroelectric switching behavior with a memory window of 2 V. The observation of the ferroelectric behavior of these materials on GaAs are promising for future GaAs devices applying the unique properties of ferroelectric materials.

This work is supported by the National Science Foundation under Grant No. ECS-0238108.

- ¹F. Ren, M. Hong, W. S. Hobson, J. M. Kuo, J. R. Lothian, J. P. Mannaerts, J. Kwo, S. N. G. Chu, Y. K. Chen, and A. Y. Cho, *Solid-State Electron.* **41**, 1751 (1997).
- ²M. Passlack, J. Abrokwhah, R. Droopad, Z. Yu, C. Overgaard, S. Yi, M. Hale, J. Sexton, and A. Kummel, *IEEE Electron Device Lett.* **23**, 508 (2002).
- ³K. D. Choquette, K. M. Geib, C. I. H. Ashby, R. D. Twesten, O. Blum, H. Q. Hou, D. M. Follstaedt, B. E. Hammons, D. Mathes, and R. Hull, *IEEE J. Sel. Top. Quantum Electron.* **3**, 916 (1997).
- ⁴K. Nashimoto, D. Fork, and T. H. Geballe, *Appl. Phys. Lett.* **60**, 1199 (1992).
- ⁵E. J. Tarsa, X. H. Wu, J. P. Ibbetson, J. S. Speck, and J. J. Zinck, *Appl. Phys. Lett.* **66**, 3588–3590 (1995).
- ⁶M. Hong, M. Passlack, J. P. Mannaerts, J. Kwo, S. N. G. Chu, N. Moriya, S. Y. Hou, and V. J. Fratello, *J. Vac. Sci. Technol. B* **14**, 2297 (1996).
- ⁷S. W. Robey, *J. Vac. Sci. Technol. A* **16**, 2423 (1998).
- ⁸V. Srikant, E. J. Tarsa, D. R. Clarke, and J. S. Speck, *J. Appl. Phys.* **77**, 1517 (1995).
- ⁹J. P. Han and T. P. Ma, *Appl. Phys. Lett.* **72**, 1185 (1998).
- ¹⁰X. H. Liu, Z. G. Liu, Y. P. Wang, T. Zhu, and J. M. Liu, *Appl. Phys. A: Mater. Sci. Process.* **76**, 197 (2003).
- ¹¹S. L. Miller and P. J. McWhorter, *J. Appl. Phys.* **72**, 5999 (1992).